Journal of Biomechanics 84 (2019) 113–120

Contents lists available at ScienceDirect

Journal of Biomechanics

journal homepage: www.elsevier.com/locate/jbiomech
www.JBiomech.com

Measuring the transverse Young's modulus of maize rind and pith tissues

Christopher J. Stubbs [a], Wenhuan Sun [b], Douglas D. Cook [c]

[a] New York University, United States
[b] New York University Abu Dhabi, United Arab Emirates
[c] Dept of Mechanical Engineering, Brigham Young University, Provo, UT 84602, USA

ARTICLE INFO

Article history:
Accepted 13 December 2018

Keywords:
Young's modulus
Transverse compression
Tissue properties
Stiffness
Finite element modeling

ABSTRACT

Wind-induced bending loads frequently cause failure of maize (corn) stalks. When failure occurs, it usually manifests as transverse buckling. Because this failure mode is closely related to transverse tissue stiffness, the purpose of this study was to develop a method for measuring the transverse Young's modulus of maize stalk rind and pith tissues. Short, disc-shaped stalk segments were used for this purpose. X-ray computed tomography was used to obtain the geometry of each specimen prior to testing. Each specimen was tested in two different configurations. Computed tomography data was used to create a specimen-specific finite element model of each test specimen. Data from the first testing configuration was used in conjunction with the finite element model to determine the Young's Modulus values for each specimen. The specimen-specific finite element models provided estimates of the stress states in the stem under transverse loading, and these stress states accurately predicted the location of failure in transverse test specimens. The entire testing method was validated using data from one test configuration to predict the structural response of each specimen during the second test configuration.

1. Introduction

Maize is the world's most highly produced crop (USDA, 2018). But in spite of its economic importance, we know relatively little about the structural characteristics of this plant. Like many other plants, maize stems can be described as foam-filled tubes (Niklas, 1991b). The tough, dense outer tissue is referred to as the rind, while the much softer, foam-like tissue in the center of the stem is called pith (see Fig. 1). Both rind and pith tissues can be approximated as transversely isotropic (Stubbs et al., 2018).

The dominant mode of maize stalk failure is transverse buckling (Robertson et al., 2014, 2015). Analytical models of transverse buckling of orthotropic tubes indicate that the critical load depends upon both the longitudinal and transverse Young's Modulus values (Wegst and Ashby, 2007; Schulgasser and Witztum, 1992). For a thin-walled, hollow orthotropic cylinder, Wegst describes the critical applied moment (M) as a function of the outer radius (r), wall thickness (t), and longitudinal and transverse Young's moduli (E' and E, respectively), given by: $M = \frac{2\sqrt{2}}{9}\pi r t^2 \sqrt{E'E}$ (Wegst and Ashby, 2007).

Several methods have been developed for quantifying the longitudinal Young's modulus of plant tissues. For example, vibrational theory and beam equations have been used to infer the longitudinal Young's Modulus of plant stems (Niklas and Moon, 1988; Niklas, 1991a). Static bending tests have also been used in a similar manner using maize (Al-Zube et al., 2018; Gou et al., 2008) and other plant species (Niklas, 1997).

Several studies have also focused on measuring the transverse material properties of plant tissues. For example, Amada et al. reported both longitudinal and transverse stiffness properties of bamboo (Amada et al., 1996) as well as detailed descriptions of common composite features such as fiber volume fraction, which was related to the measured tissue properties. This composite model paradigm has helped to develop an understanding of some of the material properties of these plants, including material strengths (Rodriguez et al., 2010) and longitudinal stiffnesses (Zhang et al., 2017; Al-Zube et al., 2017). Other studies have investigated the overall structural responses of plant stems for bending (Chen et al., 2007; Gou et al., 2008; Tongdi et al., 2011) and shear loading (Chen et al., 2007).

Only a small number of studies have directly reported tissue properties of maize tissues. Longitudinal tensile testing of the maize rind and pith was reported by Zhang et al. (2016, 2017).

E-mail address: ddc971@byu.edu (D.D. Cook)

https://doi.org/10.1016/j.jbiomech.2018.12.028
0021-9290/

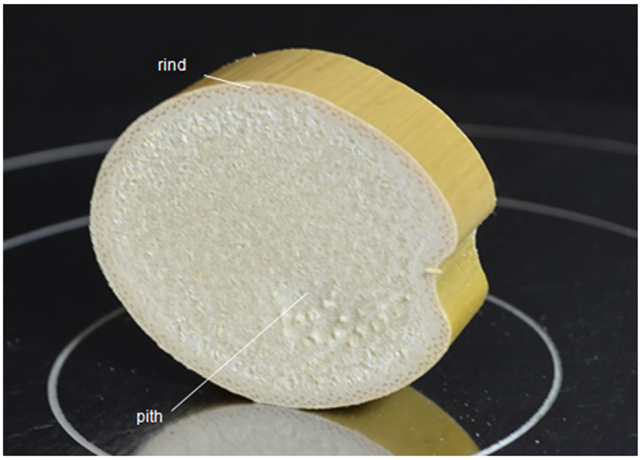

Fig. 1. A single test specimen.

However, these studies utilized dog-bone shaped specimens, which are not recommended for testing composites materials (ASTM-D5083, 2017). As an alternative, bending, compression, and tensile testing methods were developed in recent studies (Al-Zube et al., 2017, 2018). Detailed geometric data has been collected on maize stalks using x-ray computed tomography (Robertson et al., 2017).

The authors are not aware of any prior studies that have reported the transverse Young's modulus of maize tissues. Research progress on maize stalk failure is currently impeded by a lack of information about these properties. Although simple closed-form analytical solutions have been developed for single-material hollow cylinders, maize stalks are not cylindrical (see Figs. 1–3). The non-circular, non-hollow architecture is not well-suited to analytical modeling approaches. Instead, finite element models were used in this study to aid in determining the transverse Young's modulus of maize rind and pith tissues.

The purpose of this study was to (a) develop a reliable method for measuring the transverse Young's moduli of both the pith and the rind tissues in maize stems; (b) determine the validity of the method, and (c) report these tissue properties in support of future research on maize stem biomechanics.

2. Methods

2.1. Background

The length of the stem can be categorized into the nodes and the area between nodes (internodes). Internode cross sections can be divided into two main areas: the rind and the pith (Remison and Akinleye, 1978). The rind is a dense area along the outside of the cross section, while the pith is a less dense foam-like structure on the inside of the cross-section (Thompson, 1963). The cross-section is generally oval shaped, with a groove for the ear of corn to grow from (Niklas, 1998). In this study, test specimens were taken from the internodes of the stems. Internodes were cut transversely using a precision abrasive saw, into specimens with an average length of 12 mm.

2.2. Overview of testing process

Short cross-sectional specimens were tested in transverse compression (see Fig. 1) to determine the transverse stiffness of rind and pith tissues. Each specimen was tested in two orientations; with the load applied along the major diameter and with the load applied along the minor diameter, as shown in Fig. 2. The pith of each specimen was then removed, and the tests were repeated for both orientations. This resulted in four force/deformation curves for each specimen.

Specimen-specific CT scans were used to determine both the outer boundary of the specimen and the interface between the rind and the pith (Robertson et al., 2017). These boundaries were used to build a specimen-specific finite element model for each specimen. With the geometry and boundary conditions known, material properties of the finite element models were adjusted to match the experimental results. With two unknown material properties and four (4) force/deformation curves it was possible to solve for both stiffness values using two force/deformation curves. The remaining two force/deformation curves were then used to independently validate the results.

Details of the testing procedure, CT scanning, finite element model, and Young's modulus calculations are described in detail in the following sections. Specimen preparation and the testing equipment is described at the end of the Methods section.

2.3. Compression testing procedure

As shown in Fig. 2, each specimen was tested in two orientations. First, the specimen was loaded along the minor axis of the cross-section. This orientation will be referred to throughout the paper as the horizontal orientation. Second, the specimen was rotated 90 degrees and loaded along the major axis, which is referred to as the vertical orientation. Regression was performed on the resulting force-displacement curves to determine the structural stiffness of the specimen in each orientation.

Following horizontal and vertical orientation testing, the pith tissue of each specimen was carefully removed. This was somewhat challenging because the boundary between the pith and the rind is not always distinct. The best results were obtained by removing the vast majority of the pith tissue, while being careful not to inadvertently remove any of the rind tissue. This is because removal of even a small amount of rind tissue had a significant effect on structural response, but small amounts of remaining pith were found to have a negligible effect on the structural response.

2.4. CT scanning and geometry extraction

X-ray computed tomography was used to quantify cross-sectional geometry of the rind and pith regions. Specimens were scanned using an X5000 scanner (NorthStar Imaging, Rogers, MN, USA). The scanning process produced 2D cross-sectional images of the maize stems. The scanning is described in more detail in a previous study (Al-Zube et al., 2017). A custom computer program was used to extract a specimen-specific cross-sectional geometry. The program objectively identified two boundaries: the outer surface of the stem, and the boundary between the rind and pith regions.

2.5. Finite element model development

Using the CT-based geometry, a unique finite element model was created for each specimen (see Fig. 3). Each model was two-dimensional with an assumption of plane stress. The material was assumed to be transversely isotropic. The finite element models were developed in Abaqus/CAE 6.14-1. The geometry was meshed using 4-noded bilinear plane stress quadrilateral elements, using a reduced integration formulation, hourglass control, and a global seed size of 0.2 mm (Matthews, 2000; Abaqus, 2014).

Because the model was two-dimensional, and all deformation was restricted to the transverse plane, only the in-plane material properties were needed. The in-plane material properties included

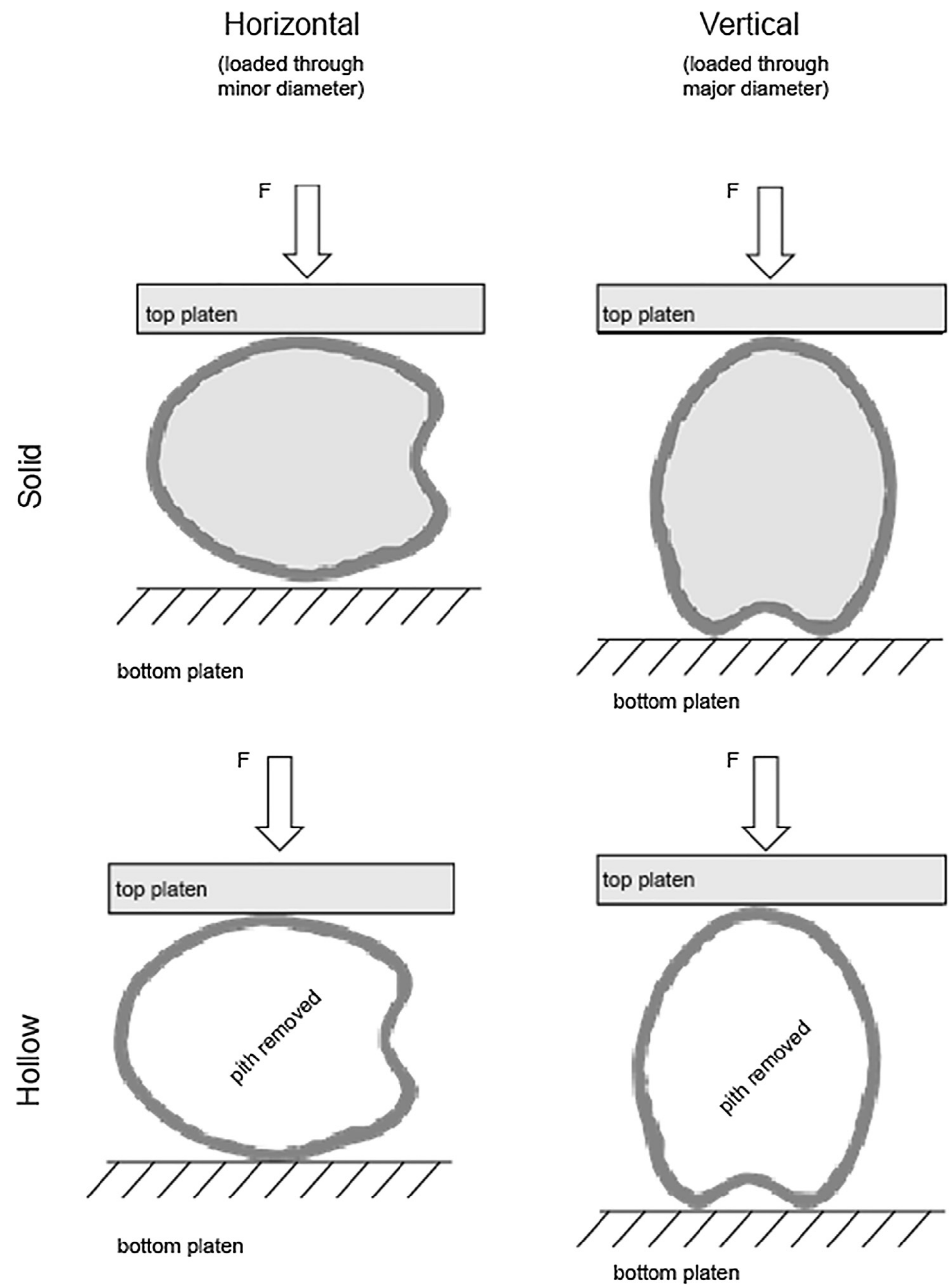

Fig. 2. The testing protocol for each specimen both with a pith (solid) and without a pith (hollow).

the transverse Young's moduli of the pith and rind regions as well as the in-plane Poisson's ratios of both materials. A sensitivity study was performed for the full range of possible Poisson's ratios. Poisson effects were found to be negligible: accounting for less than 0.2% of the structural response. As such, the Poisson's ratio was set to a moderate value of 0.25.

The same model geometry and mesh was used for all finite element simulations of a single specimen, with the orientation of the specimen matching the orientation of the testing. The bottom platen was fixed in all three degrees of freedom. The top platen was fixed in the rotational and horizontal translational degrees of freedom. The top platen was then driven to a maximum displacement of 0.2 mm in the vertical degree of freedom.

The FE models were analyzed using a non-linear, full Newton direct solver in Abaqus/Standard 6.14-1 (Abaqus, 2014). The contact between the platens and the specimen was represented by a general contact interaction with a finite-sliding formulation and a hard penalty pressure-overclosure relationship (Abaqus, 2014). Tangential friction was used to aide in convergence with a negligibly small coefficient of friction (Abaqus, 2014). No strain-free overclosure adjustments were made.

2.6. Determination of Young's modulus

The hollow model required only one material property: the Young's Modulus of the rind. In addition, the relationship between Young's modulus and the structural stiffness of the model was found to be linear. The secant method (Fausett, 2008) was used to solve for the Young's modulus value that provided agreement between the structural stiffness of the model and the structural stiffness of the specimen, as measured experimentally. In all cases,

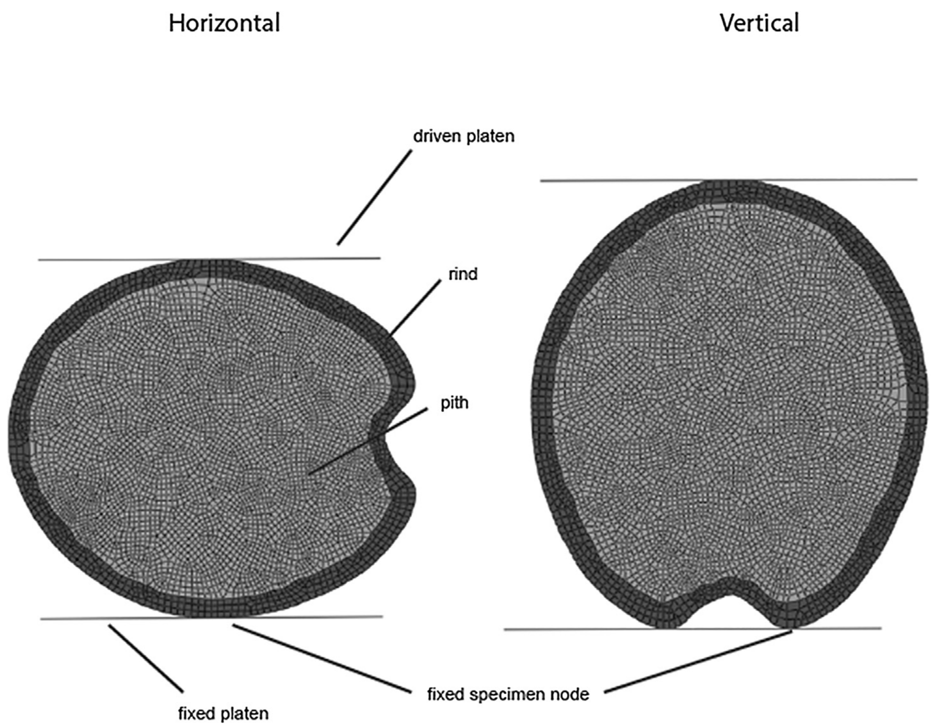

Fig. 3. A meshed finite element assembly for the horizontal (left) and vertical (right) analyses.

the structural stiffness of the finite element model matched the hollow specimen stiffness within ±1%.

Once the rind Young's modulus was known, the Young's modulus of the pith could be determined. But in contrast to the hollow model, the structural stiffness of the solid model was nonlinearly dependent upon the Young's Modulus of the pith tissue. The secant method was used to adjust the Young's Modulus of the finite element model until it matched the solid specimen stiffness within ±1%.

2.7. Validation

As previously discussed, the rind and pith Young's modulus values were obtained using only data from horizontal tests. Validation was of the method was performed by using these Young's moduli values and the finite element model of each specimen to predict each specimen's structural stiffness in the vertical orientation. Comparisons between the predicted structural stiffness and experimentally measured structural response from completed the validation process.

2.8. Stem specimens

Dried commercial hybrid maize stems were used as test specimens for this study. Stems were cut just above the ground and just above the ear node immediately before harvest. To prevent fungal growth, stems were placed in forced-air dryers to reduce stem moisture to approximately 10–15% moisture by weight, which closely mimics the state of stems in the field just prior to harvest. Only stems found to be free of disease and pest damage were included in the study.

2.9. Specimen preparation

To test the applicability of the methodology for a broad range of geometries, stems of differing cross-sectional size were selected for testing. Individual test specimens were cut from regions of each stem where cross-sectional variation was minimal. Each test specimen was cut from the stem using a precision abrasive saw, and test specimens were typically 10–12 mm in length. A total of 20 specimens were tested from 4 stems.

2.10. Compression testing equipment & procedure

Compression tests were performed using a universal testing machine (Instron 5965, Instron Corp., Norwood, MA, USA). Loads were measured with a 5 kN Instron load cell. Instrumentation control and data acquisition were managed with Instron software (Bluehill 3.0).

When testing biological tissues, a preload and repeated application of load cycles is commonly used to bring the specimens to a repeatable reference state. This procedure is used to reduce measurement variability and is referred to as pre-conditioning (Al-Zube et al., 2018).

For the solid specimens, an initial load of between 3 N and 10 N was applied to each solid specimen, depending on specimen size. Five loading cycles were then applied. In each loading cycle, the specimen was compressed beyond its pre-loaded state by 0.2 mm, and then the platens were retracted until the initial load was restored. The first four cycles were used as conditioning cycles. Only data from the fifth cycle were employed in the follow-on calculations. For all tests, the displacement rate was 0.05 mm per second and the sampling frequency was 33 Hz. The testing procedure for hollowed specimens was identical to that of the solid specimens, with the exception that the initial load was reduced to 0.2 N due to the decreased load-bearing capacity of the hollow specimens.

3. Results

3.1. Force/deformation and structural stiffness values

Force-deflection curves for each specimen were linear in nature. Linear regression on the data was used to extract specimen stiffness during the loading phase, with a coefficient of determination (R^2) typically above 0.99.

Structural stiffness values (N/mm) were normalized by the specimen length to obtain the normalized structural stiffness (N/mm^2) for each specimen. As expected, specimens exhibited higher stiffness in the vertical orientation. Hollow specimens had a stiffness values that were more than one order of magnitude lower than the solid specimens. The distributions of normalized structural stiffness values for each test are shown in Fig. 4.

3.2. Tissue stiffness values

The Young's Modulus of the rind tissue was found to have a mean value of 0.85 GPa and standard deviation of 0.39 GPa. The pith had a mean Young's Modulus value of 0.026 GPa and standard deviation of 0.01 GPa. The distributions of these stiffness values are shown in Fig. 5.

As a point of comparison, the transverse Young's modulus of the rind was found to be similar to previously reported transverse Young's modulus values of wood: spruce and pine (Gibson, 2012). The transverse Young's modulus of the pith is slightly less than the transverse modulus of balsa wood (Gibson, 2012).

3.3. Validation

The Young's moduli determined in the horizontal orientation were used to predict each specimen's structural response in the vertical orientation. The structural stiffness values predicted by the model were then compared to the experimentally measured structural stiffness values in the vertical orientation. Using a line of best fit, the finite element predictions were reasonably well correlated with the experimental data ($R^2 = 0.84$ for the hollow specimens, and $R^2 = 0.57$ for the solid specimens, as shown in Figure 6). A much more restrictive approach is to calculate the R^2 values based on an imposed 1:1 line. The correlations were somewhat lower under this model, but were still significantly correlated ($R^2 = 0.72$ for the hollow specimens, and $R^2 = 0.46$ for the solid specimens).

This validation approach provides intra-specimen validation; that is to say that the Young's moduli values calculated in one testing configuration can accurately predict the overall structural behavior – and force-displacement curve – of the specimen in a different testing configuration. This validation approach is used to avoid the issue of inter-specimen validation, where the inter-specimen variance in the measured values of biological specimens can obfuscate the reliability of the experimental approach.

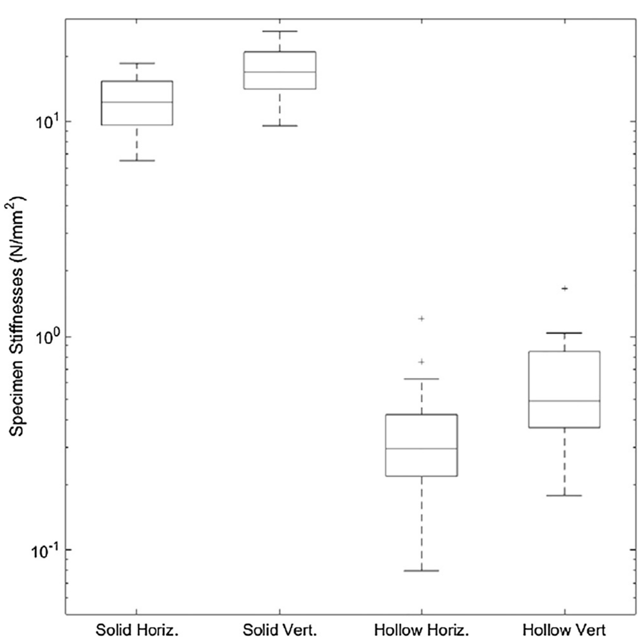

Fig. 4. Experimentally obtained structural stiffnesses by configuration (n = 20).

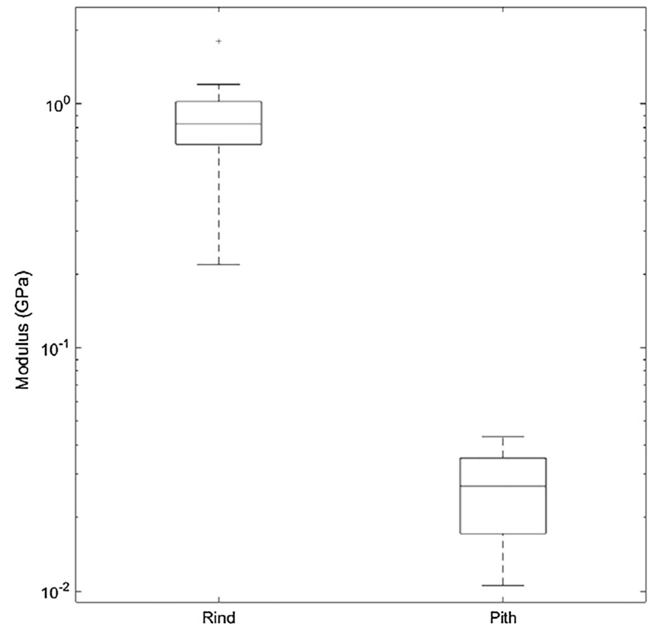

Fig. 5. Rind and pith Young's modulus distributions.

3.4. Estimated stress state

With the specimen-specific Young's moduli of the pith and rind determined, the stress state can be estimated. Although this approximation does not capture the microscopic stress concentrations, it can provide insight into the structural reaction of the stem under transverse loading, where failure is likely to occur, and why. Finite element models predicted that the maximum stresses in the pith tend to split the pith between the platen-specimen contact points (see Fig. 7). This is in agreement with what is seen under testing to failure (Zuber and Grogan, 1961; Thompson, 1963; Robertson et al., 2015) (See Fig. 8).

In Fig. 7, the finite element model is overlaid on photographs from the physical specimen testing. As an additional qualitative confirmation of the method, it should be noted that the deflected shape of the finite element analysis closely matches the deflected shape of the specimen while being tested.

3.5. Covariance of rind and pith values

The Young's moduli of the rinds were compared to the Young's moduli of the piths. Contrary to our expectations, no correlation was found between the rind and pith Young's moduli of the specimens tested in this study ($R^2 = 0.01$).

This observation suggests that these tissues serve different structural purposes. For instance, the stiffness and strength of the rind tissue may be determined in response to bending loads, while the pith may be designed to resist ovalization, thus preventing Brazier buckling (Schulgasser and Witztum, 1992).

4. Discussion

Throughout the development of this methodology, acquired valuable insights into the factors that affect test results of this kind.

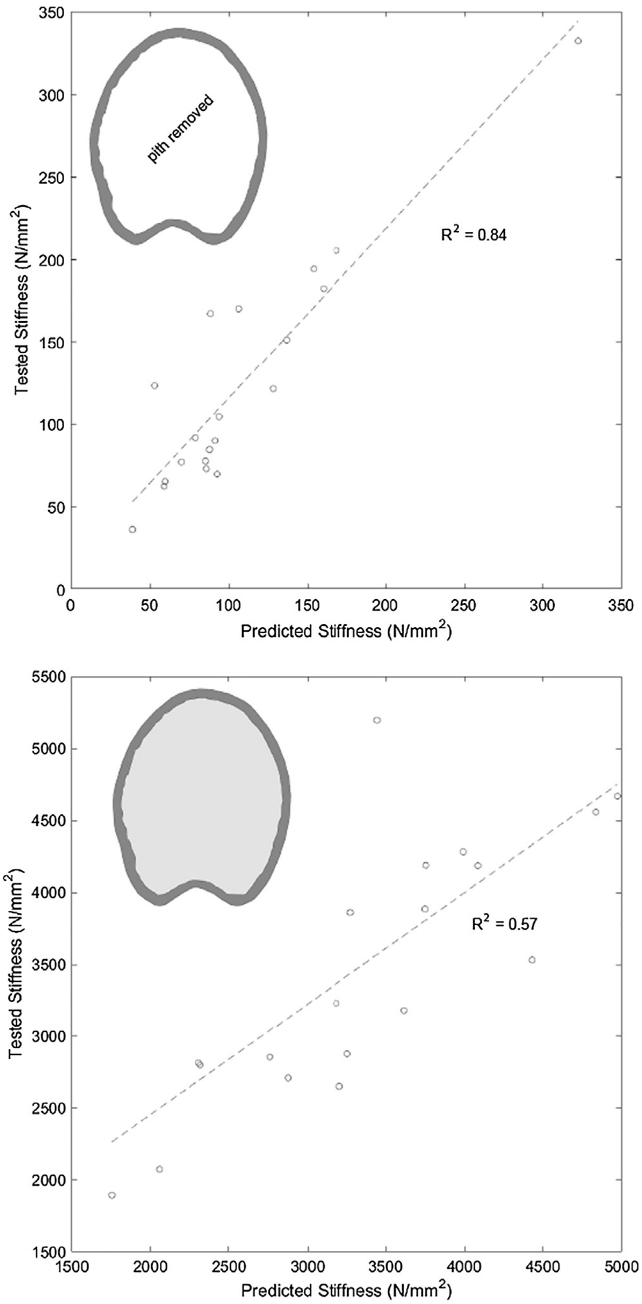

Fig. 6. Structural stiffness values as obtained by finite-element model (horizontal axis) and experimental measurements (vertical axis). Note that finite element models were created using only data from horizontal tests (not depicted in this figure). Top panel: hollow specimens; bottom panel: solid specimens.

For example, the method was varied by changing specimen lengths, cutting methods, testing configurations, and rind-pith delineation determinations. While the full details of each attempted approach is beyond the scope of this article, the most important issues are discussed below.

4.1. Sensitivity to geometry

Specimen lengths were varied from 8 mm to 17 mm to investigate the effect of specimen length. While no correlation was found between methodology accuracy and specimen length ($R^2 = 0.07$). The authors observed that perpendicular cuts were more difficult to achieve with short specimens (less than 10 mm). Longer specimens could be cut more reliably, but exhibited slight longitudinal variation in cross-sectional shape and size. This effect cannot be captured by a 2-dimensional finite element model and thus introduces discrepancies into the method. Specimen lengths of 10–12 mm were found to produce the most reliable results.

4.2. Correlation of test and validation sets

The correlation between predicted and measured stiffness was higher for hollow models. This is because only one stiffness-matching process was required for hollow models, and because the hollow model was found to have a more linear response than the solid model. Solid model predictions relied upon both rind *and* pith tissue matching, and was therefore correlated less closely with measured data.

We can draw several conclusions from these results. First, the method presented above is at least somewhat reliable since model predictions of both hollow and solid models are statistically significant. Second, the Young's modulus values of the pith tend to be more accurate and reliable than the Young's modulus values of the pith material. Third, because the method relied upon assumptions of linearly elasticity and transverse isotropy, these assumptions appear to be appropriate for these types of maize stem specimens.

Since the process itself has been validated, averaging the results of Young's modulus values obtained through both horizontal-orientation testing and vertical-orientation testing could likely lead to Young's modulus values that are even more accurate, but this approach (a) cannot be independently validated, and (b) is likely impractical for most situations.

4.3. Practical suggestions for future researchers

Various cutting methods were used to section the stems. Miter saws, table saws with different blades, chop saws, hand sanding, and grinding were all found to be unsatisfactory. This was because specimens either had cuts that were not perpendicular to the test contact surface, were not repeatable, exhibited high levels of variation, or took too much time to complete. The final method used was to cut the specimens with an TechCut 5 precision high speed saw Allied High Tech Products, Inc., Rancho Dominguez, CA). The pith was then removed using a Dremel tool with an abrasive sanding wheel and/or milling bit attachment. We found that it was important to avoid removing any rind tissue, as this would adversely affect results. The entire method achieved consistent results, and allowed a single specimen to be machined, tested in the solid configuration, milled, tested in the hollow configuration, and analyzed within approximately 30 min.

Results were found to be highly sensitive to geometry. While both visible-light photography and CT scanning were attempted, only the CT scan approach provided reliable results.

A number of limitations are present in the method presented. First, all experiments were performed on a set of mature, dried maize plants. Second, the method is time consuming. The specimen preparation and testing required approximately 30 min for each specimen, the CT scanning requires approximately an hour, and the finite element model development and analysis requires approximately 30 min. These time-consuming efforts can be partially mitigated, as the CT scanning can be done on more than one specimen at a time, and much of the finite element modeling and analysis can be automated. Finally, because the Young's modulus of the rind is calculated and then used to determine the Young's modulus of the pith, the error in the Young's Modulus of the pith is compounded by the error of the Young's modulus of the rind. As such, the estimated value for the Young's modulus of the rind are more accurate that the estimated value for the Young's modulus of the pith.

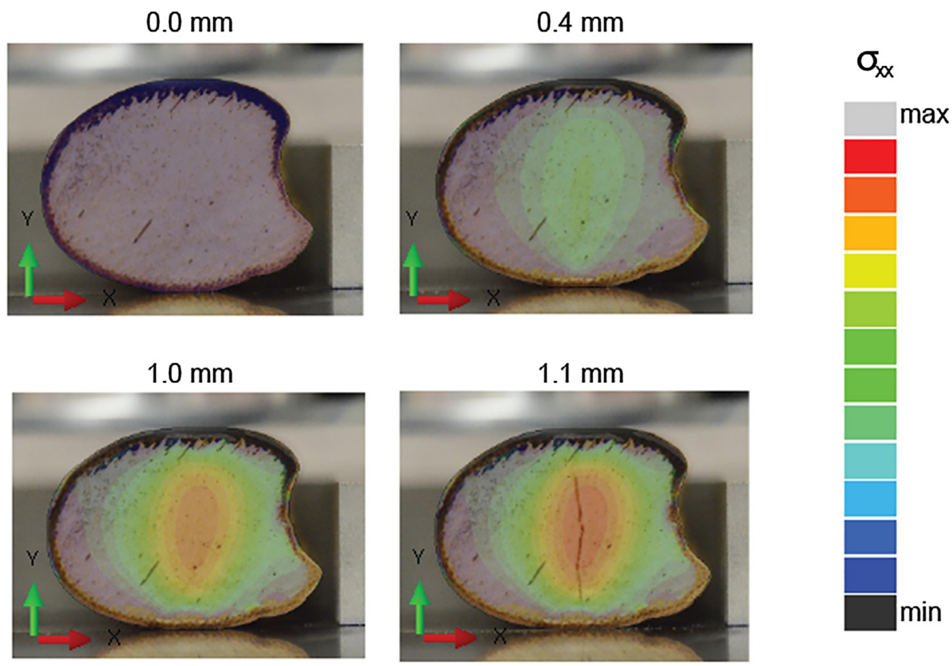

Fig. 7. X-direction normal stresses overlaid on specimen photographs at displacements from 0.0 mm to 1.1 mm. Splitting of the pith occurred at an applied deformation of 1.1 mm and occurred near the region of highest predicted stress.

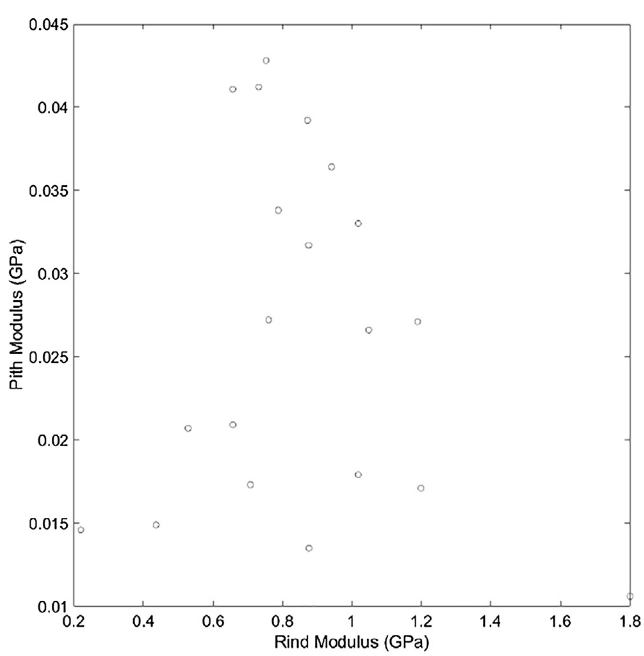

Fig. 8. Rind Young's modulus vs. pith Young's modulus.

5. Conclusions

A method was developed for determining the transverse Young's Modulus value of rind and pith tissues of maize. The method involved the physical testing of short, disc-shaped specimens from the internode region of the stem. Transverse loads were applied to these specimens while measuring the structural response of each specimen in both solid and hollowed configurations. A two-material finite-element model was then used to represent the structural response of each internodal maize specimen. Young's modulus values were obtained by matching the response of the model to the actual response of the specimens.

The method was validated by using these Young's Modulus values to predict the structural response of each specimen in a different physical orientation. Predicted values were correlated with the values obtained experimentally. This method for obtaining Young's Modulus values was found to be reliable and insensitive to cross-sectional geometry, rind thickness, stem size, and specimen testing orientation. To the author's knowledge, this paper represents the first reported data on the transverse Young's modulus of maize stem tissues.

This method can used to assess the Young's Modulus of rind and pith tissues of maize stems, and may also have application to similar tests for sorghum, sugar cane, and other plants with similar structural features.

Acknowledgements

This research was supported by Monsanto Company, the USA National Science Foundation (Award # 1400973), the Core Technology Platform Resources at New York University–Abu Dhabi, and Brigham Young University.

Conflict of interest statement

None of the authors have any conflict of interest to report.

Authors' contributions

All authors were fully involved in the study and preparation of the manuscript. The material within has not been and will not be submitted for publication elsewhere.

References

Abaqus 6.14 Documentation, 2014 abaqus.software.polimi.it/v6.14/index.html.
Al-Zube, L.A., Robertson, D.J., Edwards, J.N., Sun, W., Cook, D.D., 2017. Measuring the compressive modulus of elasticity of pith-filled plant stems. Plant Methods 13 (1), 99.
Al-Zube, L., Sun, W., Robertson, D., Cook, D., 2018. The elastic modulus for maize stems. Plant Methods 14 (1).

Amada, S., Munekata, T., Nagase, Y., Ichikawa, Y., Kirigai, A., Zhifei, Y., 1996. The mechanical structures of bamboos in viewpoint of functionally gradient and composite materials. J. Compos. Mater. 30 (7), 800–819.
ASTM-D5083, 2017. Standard Test Method for Tensile Properties of Reinforced Thermosetting Plastics Using Straight-Sided Specimens. ASTM International, West Conshohocken, PA (Accessed 18 Jan 2018 http://www.astm.org).
Chen, Y., Chen, J., Zhang, Y., Zhou, D., 2007. Effect of harvest date on shearing force of maize stems. Livestock Sc. 111 (1–2), 33–44.
Fausett, Laurene V., 2008. Applied Numerical Analysis Using MATLAB. Pearson Prentice Hall.
Gibson, L.J., 2012. The hierarchical structure and mechanics of plant materials. J. Royal Soc. Inter. 9 (76), 2749–2766.
Gou, L., Ming, Z., Jian-Jian, H., Bin, Z., Tao, L., Rui, S., 2008. Bending mechanical properties of stalk and lodging-resistance of maize (Zea mays L.). Acta Agronomica Sin. 34 (4), 653–661 (In Chinese).
Matthews, F.L., 2000. Finite Element Modelling of Composite Materials and Structures. CRC Press.
Niklas, K.J., Moon, F.C., 1988. Flexural stiffness and modulus of elasticity of flower stalks from allium sativum as measured by multiple resonance frequency-spectra. Am. J. Bot. 75 (10), 1517–1525.
Niklas, K.J., 1991a. The elastic-moduli and mechanics of populus-tremuloides (salicaceae) petioles in bending and torsion. Am. J. Bot. 78 (7), 989–996.
Niklas, K., 1991b. Bending stiffness of cylindrical plant organs with a 'core-rind' construction: evidence from Juncus effusus leaves. Am. J. Bot. 78 (4), 561.
Niklas, K., 1997. Relative resistance of hollow, septate internodes to twisting and bending. Ann. Bot. 80 (3), 275–287.
Niklas, K., 1998. Modes of mechanical failure of hollow. Septate Stems. Ann. Bot. 81 (1), 11–21.
Remison, S., Akinleye, D., 1978. Relationship between lodging, morphological characters and yield of varieties of maize (Zea mays L.). J. Agric. Sci. 91 (03), 633.
Robertson, D., Smith, S., Gardunia, B., Cook, D., 2014. An improved method for accurate phenotyping of corn stalk strength. Crop Sci. 54 (5), 2038.
Robertson, D., Julias, M., Gardunia, B., Barten, T., Cook, D., 2015. Corn stalk lodging: a forensic engineering approach provides insights into failure patterns and mechanisms. Crop Sci. 55 (6), 2833.
Robertson, D., Julias, M., Lee, S., Cook, D., 2017. Maize stalk lodging: morphological determinants of stalk strength. Crop Sci. 57 (2), 926.
Rodriguez, M., Rodriguez, A., Bayer, J., Vilaseca, F., Girones, J., Mutje, P., 2010. Determination of corn stalk fibers' strength through modeling of the mechanical properties of its composites. BioResources 5 (4).
Schulgasser, K., Witztum, A., 1992. On the strength, stiffness and stability of tubular plant stems and leaves. J. Theor. Biol. 155 (4), 497–515.
Stubbs, C.J., Baban, N.S., Robertson, D.J., Alzube, L., Cook, D.D., 2018. Bending stress in plant stems: models and assumptions. In: Geitmann, A., Gril, J. (Eds.), Plant Biomechanics. Springer, Cham.
Thompson, D., 1963. Stalk strength of corn as measured by crushing strength and rind thickness. Crop Sci. 3 (4), 323.
Tongdi, Q., Yaoming, L., Jin, C., 2011. Experimental study on flexural mechanical properties of corn stalks. In: 2011 International Conference on New Technology of Agricultural.
USDA, 2018. World Agricultural Supply and Demands Estimates. World Agricultural Outlook Board. ISSN: 1554–9089.
Wegst, U.G., Ashby, M.F., 2007. The structural efficiency of orthotropic stalks, stems and tubes. J. Mater. Sci. 42 (21), 9005–9014.
Zhang, L., Yang, Z., Zhang, Q., Zhu, X., Hu, H., 2017. Mechanical behavior of corn stalk pith: an experimental and modeling study. Agric. Eng. 51 (1).
Zhang, L., Yang, Z., Zhang, Q., Guo, H., 2016. Tensile properties of maize stalk rind. BioResources 11 (3), 6151–6161.
Zuber, M., Grogan, C., 1961. A new technique for measuring stalk strength in corn. Crop Sci. 1 (5), 378.